Title: Systemic calcitonin gene-related peptide (CGRP) modifies auditory and vestibular endorgan electrical potentials, and increases auditory and vestibular hypersensitivities

Abbreviated Title: CGRP's effect on inner ear endorgan and behavior

Authors: Shafaqat M. Rahman[1], Benjamin Liang[1], Stefanie Faucher[1], Elana Fine[1], Raajan Jonnala[1], Joseph C. Holt[2,3], Choongheon Lee[3], Anne E. Luebke[1,2*]

Affiliations:

[1]University of Rochester, Department of Biomedical Engineering, Rochester, NY 14627

[2]University of Rochester Medical Center, Department of Neuroscience, Del Monte Institute of Neuroscience, Rochester, NY 14642

[3]University of Rochester Medical Center, Department of Otolaryngology, Rochester, NY 14642

*Corresponding author: Anne E. Luebke, aluebke@ur.rochester.edu

Conflict of interest statement: The authors declare no competing financial interests.

Acknowledgments: This work was fully supported by NIH R01DC017261 (AEL).

Abstract:

Migraine is a severe and chronic neurological disorder that affects ~18% of people worldwide, the majority being female (3:1). It is characterized by recurrent, debilitating headaches and heightened sensory sensitivities. People with migraine may also experience a heightened motion sensitivity that leads to episodes of vertigo and imbalance, termed vestibular migraine (VM). Calcitonin gene-related peptide (CGRP) is implicated in migraine and is believed to act on brain meninges or in subcortical CNS structures, and CGRP-based antagonists have shown efficacy for migraine treatment. CGRP also signals at efferent synapses of the cochlea and vestibular endorgans, but it is unclear if exogenous CGRP can modulate inner ear function at the endorgan level and cause heightened behavioral responses consistent with VM. We tested if intraperitoneally (IP) delivered CGRP to wildtype mice can modulate endorgan potentials to sound [via auditory brainstem responses (ABRs)] and jerk stimuli [via vestibular sensory evoked potentials (VsEPs)]. We also assessed behavioral measures of phonophobia [acoustic startle reflex (ASR)] and static imbalance [postural sway-center of pressure (CoP)] after IP CGRP, and observed female mice exhibited heightened sensitivities to IP CGRP in all assays. Male mice showed similar auditory sensitivity and endorgan effects to CGRP, but systemic CGRP did not modify male postural sway as it did in females. In conclusion, we show that systemically delivered CGRP modulates activity of the auditory and vestibular endorgan responses and elicits behavioral effects that are consistent with symptoms in a disorder like VM.

Introduction:

Migraine is a debilitating chronic neurological disorder that is listed by the World Health Organization (WHO) as the most debilitating neurological disorder worldwide and is estimated to affect 18% of women and 6% of men (Goadsby, Lipton, & Ferrari, 2002; Lipton et al., 2007). About 42% of people with migraine have a vestibular component causing balance problems and dizziness (Kuritzky, Toglia, & Thomas, 1981; H. Neuhauser, Leopold, von Brevern, Arnold, & Lempert, 2001; H. K. Neuhauser, 2007, 2009), termed vestibular migraine (VM). VM is a major cause of vertigo in dizziness clinics (Kayan & Hood, 1984) and patients with migraine, and especially VM, exhibit a heightened sense to sound and motion (Ashkenazi, Mushtaq, Yang, & Oshinsky, 2009; Lopez-Escamez et al., 2014). Despite migraine and VM's prevalence, the pathophysiology remains uncertain (Lempert et al., 2022; Lempert et al., 2012).

Calcitonin gene-related peptide (CGRP) is intensively studied for its role in migraine's sensory hypersensitivities (A. F. Russo, 2015). CGRP levels are elevated during migraine, and normalization of CGRP levels is associated with the relief of headache pain which is thought to act at either brain meninges or the PNS (Goadsby et al., 2002; Juhasz et al., 2005; Lassen et al., 2002)) . CGRP also signals at efferent synapses of the cochlea and vestibular endorgans, so we questioned if elevated CGRP levels in migraine could directly affect the inner ear (Dickerson, Bussey-Gaborski, Holt, Jordan, & Luebke, 2016; Luebke et al., 2014; Maison, Emeson, Adams, Luebke, & Liberman, 2003). We also questioned if increases in systemic CGRP can cause behaviors suggestive of heightened auditory and vestibular sensitivities consistent with VM.

In this study, we tested wildtype C57BL/6 mice to determine if there is a change in endorgan potentials to sound (measured using auditory brainstem responses - ABRs) and jerk stimulus (measured using vestibular sensory evoked potentials - VsEPs) after an intraperitoneal (IP) CGRP injection. We also assessed corresponding behavioral measures of phonophobia (acoustic startle reflex – ASR) and imbalance (postural sway/center of pressure - CoP) after an IP CGRP injection.

Methods:

Animals

C57BL/6J mice were obtained from Jackson Laboratories (JAX #664) and were housed under a 12-hour day/night cycle under the care of the University Committee on Animal Resources (UCAR) at the University of Rochester. Mice were housed together in cages (5 mice per cage) with *ad libitum* access to food, water, and nesting and bedding materials. A total of 74 mice (37F/ 37M) were used for these studies, which were powered sufficiently to detect male/female differences. Before experimentation, mice were equilibrated in the testing room controlled for an ambient temperature between 22-23°C for at least 30 minutes and remained in this room until completion of experiments. Injections occurred after the equilibration period. Mice used during behavioral experiments were returned to the vivarium, while mice used for ABR/VsEP experiments were euthanized after testing. Mice tested were between 2.3 - 6 months of age. This age range in mice correlates to 20-30 years in humans, which is within the age range that patients develop migraine symptoms (Lessem, 2018). All animal procedures were approved by the University of Rochester's IACUC committee and performed in accordance with NIH standards. Moreover, the experimental protocols followed the guidelines for Animal Research Reporting In Vivo Experiments (ARRIVE) (McGrath & Lilley, 2015).

VsEP and ABR Protocol

C57BL/6J mice were anesthetized with IP urethane/xylazine (1.2 g/kg/20 mg/kg). VsEP and ABR recording methods have been described in detail elsewhere (Lee, Holt, & Jones, 2017). Briefly, to record VsEP and ABR, subcutaneous electrodes were placed on the midline over the nuchal crest (G1), behind the right pinna (G2), and on the hip (ground). A noninvasive head clip was used to secure the mouse's head to an electromechanical shaker. During VsEPs, the shaker delivered a transient (jerk) head translation in the naso-occipital axis (± X). To confirm the absence of auditory responses during VsEP testing, a binaural forward masker (intensity: 92 dB SPL; bandwidth: 50~50 kHz) was presented with the use of a free-field speaker (FF1, TDT). For ABR recordings, the same electrodes were used to record ABRs, which were evoked by a single rectangular voltage pulse of 0.03 ms duration (corresponding to 33 kHz cut-off frequency). These click stimuli were presented via a free-field

speaker, which was the same driver for acoustic masking during the VsEP recording. A noninvasive rectal thermometer or thermistor was used to monitor the animals' core temperature at 38.0 ± 0.2°C. The standard signal averaging technique described in previous studies (Lee et al., 2017) was used to record both VsEP and ABR, as shown in **Fig. 1A**. Recordings of both ABRs and VsEPs were made in a soundproof booth. Both ABRs at maximal intensity 100 dB SPL, and VsEPs at maximal intensity +6 dB re: 1 g/ms, were recorded as a stable baseline before a single IP injection of either vehicle control (PBS) or 0.1 mg/kg CGRP was given. Control amplitude and latencies are depicted as the averages of the 2-3 measurements taken during baseline before injection. Following single IP injections of either vehicle or CGRP, ABR and VsEP recordings were continuously measured where significant shifts in ABR and VsEP responses were first observed in 10 mins and then reaching a plateau within 15 mins of drug injection (post-CGRP; data not shown). Thus, amplitudes and latencies depicted as post-saline/post-CGRP are averages of the 2-3 measurements taken after 20-30 min post-injections.

Drug administration

Injections were performed intraperitoneally (IP) with a 30-gauge insulin syringe. Dulbecco PBS served as the vehicle control. IP CGRP was prepared at 0.1 mg/kg (rat α-CGRP, Sigma). Injection volumes were calibrated so that each animal received 1 injection per testing day at ~100 ul. For behavioral experiments, mice were tested ~20 minutes after IP delivery of either vehicle or CGRP.

Behavioral test of phonophobia: Acoustic startle reflex (ASR)

We used the acoustic startle response (ASR) to assess heightened sound sensitivity as a surrogate behavior for phonophobia in mice. Experiments were conducted within a sound-attenuating room (IAC, Bronx, NY) with Sonex foam lined walls. Mice were placed individually in a wire-mesh cage that is 5 cm wide, 7 cm long, and 4 cm high, and having free sound penetration. The testing cage was oriented so that the mouse faced a Tucker Davis ES2 electrostatic speaker (Masker Speaker) located 46 cm directly in front of the mouse's head (60dB BBN). The startle speaker was a Radio Shack tweeter that was suspended 15 cm above the mouse (80-130 dB). The acoustic startle speaker and its supports, the pedestal, acrylic shelf, and the table on which the apparatus was placed were all covered with echo

absorbing foam and carpeting. Force of the ASR was transduced by an accelerometer and amplitude scored as integrated root mean square voltage for 100 ms after delivery of the ASR. Experimental stimuli were controlled, and responses were recorded using custom MATLAB (MathWorks) software. There were 12 conditions in this session, with startle stimuli ranging from 80 to 130 dB SPL, and delivered either in silence or in a continuous background noise. When present, background noise was on for the duration of the inter-trial interval and broadcasted from the masker speaker, as shown schematically in **Fig. 2**. Mice were first tested ~20-30 min after a vehicle (saline) injection, and then one week later, the same mice were retested 30 min after an IP injection of rat αCGRP (Sigma). The testing duration is 45 min/mouse, and ASR has excellent test/retest reliability (Allen & Luebke, 2017).

Behavioral test of postural sway

Postural sway was examined using the center of pressure (CoP) test which acts as surrogate behavior for static imbalance in mice. Mice were weighed and placed on a force plate designed to measure forces in the X, Y, Z axes and moments in the XY, YZ, and XZ directions. We used the AMTI Biomechanics Force platform (model HEX6x6) and AMTI automated acquisition software to obtain forces and moments and then MATLAB code was used to calculate CoP measures based on a confidence ellipse enclosing 95% of the CoP trajectory values recorded in a single trial. During a given test, mice were first allowed to freely maneuver on the force plate for 2-5 minutes to acclimate to the novel environment. An accessory plexiglass guard was placed around the force plate to prevent mice from moving off the test plate. After acclimation, ~ 10 baseline trials were taken of mice with each trial indicating a CoP area (resolution per CoP measurement: 300 samples per second). These trials were taken when the mouse was not moving and its four paws were touching the force platform. To assess the effect of a vestibular challenge (VC), mice were then subjected to a constant orbital rotation of 125 rpm for 5 minutes, and were placed back onto the force platform. After a five-minute recovery period, an additional 10 trials were recorded of the mouse's sway to determine post-VC effects on CoP as schematized in **Fig. 3**. Mice were first tested after systemic delivery of IP vehicle (20 min after injection), with sway measured before and after the VC. Four days after vehicle testing, the same mice were injected with IP CGRP and were tested again 20 minutes after injection (timing correlated with

endorgan potential changes in ABRs and VsEPs). While systemic CGRP's effect is believed to dissipate two to three hours post–injection, we retested after four days to avoid any residual dizziness due to VC or lingering CGRP effects. We staggered sequence of IP injections in some animals by injecting CGRP followed by vehicle testing on the next day. We also injected vehicle 2x to assess test/retest reliability and saw no differences. Unreasonably large CoP values (> 15 cm^2) suggested mice were either moving/grooming during the trial or that they were at the edge of the force plate, and those values were excluded based on a 10% ROUT analysis (GraphPad Prism 9.5). Even with values excluded, a minimum of eight different 95% ellipses were computed per mouse in each testing condition.

Statistical Analyses

All statistical analyses were conducted in GraphPad Prism 9.5. Analyses were conducted separately in females and males. Repeated measure ANOVA (RM-ANOVA) and paired t-tests were the primary statistical tools. Tukey post hoc analysis was used to assess treatment differences in females or males, and Bonferroni post hoc analysis was used to assess treatment differences between sexes. Significance was set at $p < 0.05$ for all analyses. Animals are repeatedly tested to account for interanimal variability. We did not exclude animals based on their averaged 95% confidence ellipse area as there will be individual variation.

Results:

Systemic CGRP's effects on ABR

Representative traces are shown for ABR recordings in female and male C57BL/6J mice **(Fig. 1B, C)**. Female control ABR wave 1 (P1) amplitudes (n = 6) were computed to be 1.74 ± 0.20 μV and increased to 2.08 ± 0.21 μV after IP CGRP (one-tailed paired t-test; t, df = 3.94, 5; p = 0.01). In males, control ABR wave 1 amplitudes (n = 7) were computed to be 2.78 ± 0.26 μV and changed to 2.89 ± 0.25 μV after IP CGRP (one-tailed paired t-test; t, df = 1.02, 6; not significant) **(Fig. 1F)**. Wave 1 ABR amplitudes were normalized so that post-CGRP measurements highlight the change in amplitude from their respective control measurements (Δ wave1 amplitude) **(Fig. 1G)**. When sexes are pooled (n = 13),

a significant Δ increase of 0.22 ± 0.08 μV was observed in wave 1 amplitudes due to IP CGRP (one-tailed paired t-test**;** *t, df* = 2.89,12**;** p = 0.01). In parallel, a different group of mice were tested to examine the effects of the vehicle control, IP PBS, on the ABR response (**Supplementary Fig. 1A, B**). IP vehicle induced negligible changes in ABR wave 1 amplitude, as changes were regarded not significant in females (n = 4) or males (n = 4). Wave 2-1 ABR latencies were calculated as the difference between P2 and P1 latencies for control and post-CGRP; however, no differences were observed in latencies **(Fig. 1H).** IP vehicle also had no effects on Wave 2-1 ABR latencies (**Supplementary Fig. 1C)**.

IP CGRP's effects on VsEPs

Similar to ABR tests, representative traces are shown for VsEP recordings in females and males (**Fig. 1D, E).** Female P1-N1 VsEP control amplitudes (*n* = 6) were computed to be 0.68 ± 0.06 μV and were reduced to 0.55 ± 0.06 μV after IP CGRP (one-tailed paired t-test; *t, df* = 1.96, 5; *t* (*p* = 0.054)) **(Fig. 1I)**. Likewise, male P1-N1 VsEP control amplitudes (*n* = 8) were computed to be 0.95 ± 0.10 μV but were reduced significantly to 0.76 ± 0.10 μV after IP CGRP (one-tailed paired t-test; *t, df* = 3.00, 7; *p* = 0.009). P1-N1 amplitudes were normalized so that post-CGRP measurements highlight the change in amplitude from their respective control (Δ P1-N1 amplitude), and both sexes were additionally pooled (**Fig. 1J**). When pooling all animals (*n* = 14), a significant Δ reduction of -0.16 ± 0.04 uV in P1-N1 amplitude is observed due to IP CGRP (one-tailed paired t-test**;** *t, df* = 3.65, 13**;** *p* = 0.002). These changes translate to an 18.9% reduction in VsEP P1-N1 amplitude in females and a 19.4% reduction in males. In contrary, IP vehicle led to insignificant changes in VsEP P1-N1 amplitude for females (n = 5) and males (n = 4) (**Supplementary Fig. 1D, E**). P1, N1, and P2 latencies were also assessed for VsEPs, and these latencies are depicted as mean ± SEM for females and males during control and post-CGRP tests **(Fig. 1K),** with no significant difference due to IP CGRP. IP PBS had no significant effects on P1, N1, or P2 latencies (**Supplementary Fig. 1F**).

CGRP's effect on sound sensitivity

Our sound sensitivity measure in the mouse model makes use of the acoustic startle response (ASR) in quiet and in background noise. Mice were assessed for the effects of IP CGRP as compared to IP vehicle (serving as baseline). Mice were first tested for their ASR in quiet and in background noise ~30 min after a vehicle (saline) injection, and then one week later, the same mice were re-tested 30 min after an IP injection of rat αCGRP (Sigma). The ASR experimental setup is illustrated in **Fig. 2 A** (quiet) and **Fig. 2D** (background noise 60 dB). In both IP vehicle and IP CGRP injected animals, an increase in ASR was detected with increasing loudness of the startle stimulus (ES). All animals tested exhibited robust startle responses (n = 6F/ 6M) to vehicle injections. When ASR was tested after IP CGRP injection and compared to IP vehicle, all animals exhibited reduced ASR thresholds in both quiet and noise. IP CGRP significantly increased sound sensitivity to the startle stimulus in quiet (**Fig. 2 B, C**) and in background noise (**Fig. 2 E, F**) in both female and male mice at all sound levels ($p < 0.0001$ quiet, $p < 0.001$ in noise).

<u>CGRP's and VC's effects on postural sway</u>

Mice were assessed for postural sway by determining center of pressure (CoP) ellipse area. An experimental timeline is shown in **Fig. 3A**. Twenty minutes after delivery of IP vehicle and without a vestibular challenge (VC), group averages of 95% ellipse areas were computed to be 0.5 ± 0.06 cm^2 for females and 0.4 ± 0.04 cm^2 for males **(Fig. 3B and C).** In Fig. 3B, we show 3 distinct 95% confident ellipse areas (3 trials) for one female mouse tested on postural sway about twenty minutes after IP vehicle administration, to give a visual of what each trial looks in respect to the location of the mouse on the platform. There is little variability in each trial regardless of where the mouse is on the platform. Similarly, three trials of a male mouse's postural sway after IP vehicle are shown in **Fig. 3C**. In **Fig. 3D**, we placed a toy mouse on the platform right at the center (0 cm/0 cm) to indicate the comparatively small 95% confident ellipse areas that are generated by a dead weight when compared to a live mouse, and this dead weight result is consistent if you place it in a different location on the force plate. The deadweights average 95% CoP ellipse area was computed to be 0.02 ± 0.0005 cm^2. A different cohort of mice (n = 10F/ 10M) was assessed for a test-retest of 95% ellipse areas after IP vehicle treatment, and testing occurred four days apart. A 2-way repeated measure ANOVA with Bonferroni post-hoc

analysis indicated no significant differences in either sex during the test-retest for females (mean difference = 0.10 ± 0.3 cm^2) or for males (mean difference = -0.14 + 0.3 cm^2) ($p > 0.99$ for either sex). In either sex, 2-way ANOVAs with Tukey post hoc analyses were used to assess the factors of CGRP and VC on 95% CoP ellipse areas in mice (n = 14F/ 10M) **(Fig. 3E). (Fig. 3E).** Differences were seen in females due to IP CGRP (F (1.00, 13.00) = 4.77, p = 0.05) and the VC (F (1.00, 13.00) = 4.49, p = 0.05). In females after IP vehicle, the VC induced higher CoP ellipse compared to pre-VC trials (p = 0.02) as shown in **Fig. 3F**. When comparing pre-VC trials, IP CGRP induced increases in female CoP areas by 0.94 ± 0.23 cm^2 compared to IP vehicle (p = 0.003) as seen in **Fig. 3G.** Females also had 0.96 ± 0.15 cm^2 higher CoP areas than males based on a separate 2-way ANOVA assessing sex differences in pre-VC, CGRP and post-VC, CGRP results (p = 0.001).

The major and minor axes of 95% ellipse areas were also analyzed with 2-way ANOVAs across the factors CGRP and VC (**Fig. 3H and I**). The major and minor axes lengths serve as correlates for anteroposterior (AP) and mediolateral (ML) sway magnitudes. A 2-way RM ANOVA on major axes indicated significant effects in females due to IP CGRP (F (1.00, 13.00) = 5.59; p = 0.03) and VC (F (1.00, 13.00) = 5.41; p = 0.04) whereas these effects were not observed in males. In comparison, ANOVAs that analyzed minor axes indicated a VC effect in only females (F (1.00, 13.00) = 7.46; p = 0.02). Tukey post-hoc indicated IP CGRP induced larger AP ellipse lengths by 0.49 + 0.10 cm in females compared to their IP vehicle trials (p = 0.001). Also, in IP vehicle-treated females, there was an increase in AP ellipse lengths during the post-VC test versus pre-VC (p = 0.02). IP CGRP-treated females exhibited greater AP lengths compared to males during pre-VC testing by 0.57 + 0.08 cm (p < 0.001). ML lengths increased after the VC in IP vehicle-treated females (p = 0.02), and IP CGRP-treated females had higher ML ellipse lengths compared to their IP vehicle response (p = 0.007). No other significant changes were observed in AP and ML sway.

Discussion

Using electrophysiological techniques (ABR/VsEP), we observed that intraperitoneally delivered CGRP modulates endorgan function in the inner ear with the maximum effect occurring ~20- 30 minutes after

injection. Exogenous CGRP increases wave 1 amplitudes of the ABR but reduces VsEP P1-N1 amplitudes, suggesting at least one action of systemic CGRP is at efferent targets of the auditory and vestibular periphery. Wave 1 is widely understood to arise respectively from the distal and proximal auditory nerve, whereas P1-N1 VsEP arise from peripheral vestibular nerve activity (Jones et al., 2011; Konrad-Martin et al., 2012). These structures begin in the inner ear and travel to the brainstem and project to the cochlear and vestibular nuclei. Yet, as suggested by other studies, CGRP and its receptor are widely distributed across the cerebellum, thalamus, and hypothalamus, and CGRP's effects in vestibular symptoms of migraine may be attributed to changes in the CNS such as the vestibulo-thalamo-cortical network (Espinosa-Sanchez & Lopez-Escamez, 2015; Lopez-Escamez et al., 2014; Warfvinge & Edvinsson, 2019).

Furthermore, we observed that systemic or IP CGRP - during this 20-to-30-minute timeframe - increased sound sensitivity in male and female C57BL/6J mice. Both the increases in ABR wave 1 amplitudes and the increased ASR responses are complementary to CGRP's effect on compound action potentials (CAPs) observed in intra-cochlear infusion of CGRP(Le Prell, Hughes, Dolan, & Bledsoe, 2021). In addition, the increased sound sensitivity and increased wave 1 ABR amplitude with IP CGRP injection parallel findings of decreased sound sensitivity and reduced wave 1 amplitude in αCGRP–null mice (Allen & Luebke, 2017; Dickerson et al., 2016; Maison et al., 2003). Thus, the auditory nerve may be hypersensitized to CGRP's effects during a migraine.

Peripheral IP injection of CGRP has been extensively studied in preclinical rodent models of migraine where it is believed to affect the PNS. For instance, peripheral IP inujection of CGRP resulted in light-aversive behaviors in WT mice (Mason et al., 2017). Additionally, peripherally administered CGRPcan produce spontaneous pain in mice as assessed by the grimace assay (Rea et al., 2018) . Our ABR and VSeP findings show that systemic CGRP does in fact reach the inner ear space. While the entry of substances into the inner ear is not strictly regulated by the rules governing entry of that same substance into the CNS, the molecular weight (i.e., size) of that substance, its solubility measures, and whether that substance is charged can influence its access to inner ear fluids, particularly following

systemic administration (Lee et al., 2021; Salt and Hirose, 2018). IP administration of AMPA receptor blockers (IEM1460 and IEM1925) has been shown to reach and modulate the inner ear despite being positively charged compounds, as evidenced by the presence of these blockers in perilymph samples and their effect in reducing CAP amplitudes (Walia et al., 2021). Furthermore, a number of charged cholinergic compounds can enter the inner ear despite their inability to cross the CNS BBB (Lee et al., 2021). We also considered that another explanation for CGRP's effects may be due to CGRP-mediated changes in inner ear blood flow (Hillerdal & Andersson, 1991; Quirk, Seidman, Laurikainen, Nuttall, & Miller, 1994), yet when CGRP was eliminated in CGRP-null mice, distortion product otoacoustic emissions (DPOAEs) which are very dependent on blood flow, were not affected (Dickerson et al., 2016). In fact, peripheral CGRP's effect on light aversion was also independent of any vasodilatory effects as CGRP=induced light-aversion was observed with normalized blood pressure (Mason et al., 2020).

We are confident that the CGRP neuropeptide when delivered intraperitoneally modulates inner ear activity, as we did not observe significant changes at wave 1/P1-N1 in a separate group of mice tested with IP PBS. We assessed IP PBS's effects at the same time frame as we studied IP CGRP and observed no significant changes from baseline ABR/VsEP responses. Notably, our finding of IP CGRP reducing VsEP P1-N1 amplitude is a novel contribution to our study, while the trend of IP CGRP enhancing ABR is consistent with another study that demonstrated a 20-30% increase in CAP amplitude following intracochlear CGRP infusion (Le Prell et al., 2021). When combining electrophysiology data from both males and females, it was observed that IP PBS decreased mean ABR wave 1 by 4.0% and mean VsEP P1-N1 by 1.0% compared to their baseline control measurements. In contrast, IP CGRP resulted in a 9.3% increase in mean ABR wave 1 and a 19.4% decrease in mean VsEP P1-N1 from their baseline control measurements. Notably, IP CGRP had a profound effect on females by increasing mean ABR wave 1 amplitudes by 19% from control . Several previous studies have shown normal saline, PBS and other vehicle solutions (DMSO, Kolliphor, and alcohol-based solutions) do not produce significant changes in VsEP/ABR responses over a duration of up to 2 hours (Lee et al., 2017; Lee & Jones, 2018, 2021) and our current IP PBS results strongly align

with these earlier findings, thus reinforcing the reliability of our findings and providing confidence that IP CGRP is modulating inner ear afferent activity.

A few studies in animal models have provided additional evidence for CGRP's role in vestibular dysfunction and sound sensitivity. Intracerebral-ventricular (ICV) injection of nitroglycerin (NTG) caused impaired balance beam walking in rats, and immunohistochemistry detected more CGRP expression in the vestibular nucleus of the NTG rat model than was observed in controls. Moreover, administration of a CGRP-receptor antagonist (olcegepant-BIBN4096BS) was shown to be effective in alleviating impaired balance beam walking (Tian et al., 2022; Zhang et al., 2020).

Our postural sway testing showed a robust sex difference, as female mice were much more affected than their male counterparts to IP CGRP. In all mice IP CGRP injection was compared to each mouse's baseline IP vehicle, with some female mice showing greater effects than others, but all showed increased postural sway to IP CGRP. It is unclear why we did not find significant changes in males during postural sway testing, yet female-specific sexual dimorphism has been observed in other preclinical assays assessing CGRP's effects in migraine, but we are the first to show such differences in a preclinical postural sway assay (Paige et al., 2022; Recober et al., 2009).

Systemic administration of small molecule blockers of the CGRP receptor called 'gepants' have been shown to enter the PNS like CGRP (Kim et al., 2022). Ongoing studies will determine if blocking CGRP receptor signaling by small molecules ('gepants") or by larger monoclonal blocking antibodies (mAbs) - that may or may not cross blood brain barrier (BBB), but are considered permeable to various peripheral ganglia - can reduce these sound and imbalance sensitivities due to CGRP (Noseda et al., 2020; Tian et al., 2022; Zhang et al., 2020). The current evidence in favor of anti-CGRP mAbs for treating VM is compelling. A prospective observational cohort study over 18 months observed significant reduction in vertigo and headache frequency in 50 VM patients treated with various anti-CGRP monoclonal antibodies (C. V. Russo et al., 2023), suggesting our preclinical findings may be directly translated to migraine patients.

References:

Allen, P. D., & Luebke, A. E. (2017). Reflex Modification Audiometry Reveals Dual Roles for Olivocochlear Neurotransmission. *Frontiers in Cellular Neuroscience, 11*. doi:10.3389/fncel.2017.00361

Ashkenazi, A., Mushtaq, A., Yang, I., & Oshinsky, M. L. (2009). Ictal and interictal phonophobia in migraine-a quantitative controlled study. *Cephalalgia, 29*(10), 1042-1048. doi:10.1111/j.1468-2982.2008.01834.x

Dickerson, I. M., Bussey-Gaborski, R., Holt, J. C., Jordan, P. M., & Luebke, A. E. (2016). Maturation of suprathreshold auditory nerve activity involves cochlear CGRP-receptor complex formation. *Physiol Rep, 4*(14). doi:10.14814/phy2.12869

Espinosa-Sanchez, J. M., & Lopez-Escamez, J. A. (2015). New insights into pathophysiology of vestibular migraine. *Front Neurol, 6*, 12. doi:10.3389/fneur.2015.00012

Goadsby, P. J., Lipton, R. B., & Ferrari, M. D. (2002). Migraine--current understanding and treatment. *N Engl J Med, 346*(4), 257-270. doi:10.1056/NEJMra010917

Hillerdal, M., & Andersson, S. E. (1991). The effects of calcitonin gene-related peptide (CGRP) on cochlear and mucosal blood flow in the albino rabbit. *Hear Res, 52*(2), 321-328. doi:10.1016/0378-5955(91)90022-2

Jones, T. A., Jones, S. M., Vijayakumar, S., Brugeaud, A., Bothwell, M., & Chabbert, C. (2011). The adequate stimulus for mammalian linear vestibular evoked potentials (VsEPs). *Hear Res, 280*(1-2), 133-140. doi:10.1016/j.heares.2011.05.005

Juhasz, G., Zsombok, T., Jakab, B., Nemeth, J., Szolcsanyi, J., & Bagdy, G. (2005). Sumatriptan causes parallel decrease in plasma calcitonin gene-related peptide (CGRP) concentration and migraine headache during nitroglycerin induced migraine attack. *Cephalalgia, 25*(3), 179-183. Retrieved from

http://www.ncbi.nlm.nih.gov/entrez/query.fcgi?cmd=Retrieve&db=PubMed&dopt=Citation&list_uids=15689192

Kayan, A., & Hood, J. D. (1984). Neuro-otological manifestations of migraine. *Brain, 107 (Pt 4)*, 1123-1142. Retrieved from http://www.ncbi.nlm.nih.gov/pubmed/6334543

Kim, M. S., Kim, B. Y., Saghetlians, A., Zhang, X., Okida, T., & Kim, S. Y. (2022). Anti-nociceptive effects of dual neuropeptide antagonist therapy in mouse model of neuropathic and inflammatory pain. *Korean J Pain, 35*(2), 173-182. doi:10.3344/kjp.2022.35.2.173

Konrad-Martin, D., Dille, M. F., McMillan, G., Griest, S., McDermott, D., Fausti, S. A., & Austin, D. F. (2012). Age-related changes in the auditory brainstem response. *J Am Acad Audiol, 23*(1), 18-35; quiz 74-15. doi:10.3766/jaaa.23.1.3

Kuritzky, A., Toglia, U. J., & Thomas, D. (1981). Vestibular function in migraine. *Headache, 21*(3), 110-112. Retrieved from http://www.ncbi.nlm.nih.gov/pubmed/6973556

Lassen, L. H., Haderslev, P. A., Jacobsen, V. B., Iversen, H. K., Sperling, B., & Olesen, J. (2002). CGRP may play a causative role in migraine. *Cephalalgia, 22*(1), 54-61. Retrieved from http://www.ncbi.nlm.nih.gov/entrez/query.fcgi?cmd=Retrieve&db=PubMed&dopt=Citation&list_uids=11993614

Le Prell, C. G., Hughes, L. F., Dolan, D. F., & Bledsoe, S. C. (2021). Effects of Calcitonin-Gene-Related-Peptide on Auditory Nerve Activity. *Frontiers in Cell and Developmental Biology, 9*. doi:10.3389/fcell.2021.752963

Lee, C., Holt, J. C., & Jones, T. A. (2017). Effect of M-current modulation on mammalian vestibular responses to transient head motion. *J Neurophysiol, 118*(6), 2991-3006. doi:10.1152/jn.00384.2017

Lee, C., & Jones, T. A. (2018). Acute blockade of inner ear marginal and dark cell K(+) secretion: Effects on gravity receptor function. *Hear Res, 361*, 152-156. doi:10.1016/j.heares.2018.02.002

Lee, C., & Jones, T. A. (2021). Effects of Several Therapeutic Agents on Mammalian Vestibular Function: Meclizine, Diazepam, and JNJ7777120. *J Assoc Res Otolaryngol, 22*(5), 527-549. doi:10.1007/s10162-021-00803-5

Lempert, T., Olesen, J., Furman, J., Waterston, J., Seemungal, B., Carey, J., . . . Newman-Toker, D. (2022). Vestibular migraine: Diagnostic criteria1. *J Vestib Res, 32*(1), 1-6. doi:10.3233/VES-201644

Lempert, T., Olesen, J., Furman, J., Waterston, J., Seemungal, B., Carey, J., . . . Newman-Toker, D. (2012). Vestibular migraine: diagnostic criteria. *J Vestib Res, 22*(4), 167-172. doi:10.3233/VES-2012-0453

Lessem, S. E. (2018). *QuickStats: Percentage of Adults Who Had a Severe Headache or Migraine in the Past 3 months, by Sex and Age Grou - National Health Interview Survey, United States, 2018*.

Lipton, R. B., Bigal, M. E., Diamond, M., Freitag, F., Reed, M. L., Stewart, W. F., & Group, A. A. (2007). Migraine prevalence, disease burden, and the need for preventive therapy. *Neurology, 68*(5), 343-349. doi:10.1212/01.wnl.0000252808.97649.21

Lopez-Escamez, J. A., Dlugaiczyk, J., Jacobs, J., Lempert, T., Teggi, R., von Brevern, M., & Bisdorff, A. (2014). Accompanying Symptoms Overlap during Attacks in Meniere's Disease and Vestibular Migraine. *Front Neurol, 5*, 265. doi:10.3389/fneur.2014.00265

Luebke, A. E., Holt, J. C., Jordan, P. M., Wong, Y. S., Caldwell, J. S., & Cullen, K. E. (2014). Loss of alpha-calcitonin gene-related peptide (alphaCGRP) reduces the efficacy of the Vestibulo-ocular Reflex (VOR). *J Neurosci, 34*(31), 10453-10458. doi:10.1523/JNEUROSCI.3336-13.2014

Maison, S. F., Emeson, R. B., Adams, J. C., Luebke, A. E., & Liberman, M. C. (2003). Loss of alpha CGRP reduces sound-evoked activity in the cochlear nerve. *J Neurophysiol, 90*(5), 2941-2949. doi:10.1152/jn.00596.2003

Mason, B. N., Kaiser, E. A., Kuburas, A., Loomis, M. M., Latham, J. A., Garcia-Martinez, L. F., & Russo, A. F. (2017). Induction of Migraine-Like Photophobic Behavior in Mice by Both Peripheral and Central CGRP Mechanisms. *J Neurosci, 37*(1), 204-216. doi:10.1523/JNEUROSCI.2967-16.2016

Mason, B. N., Wattiez, A. S., Balcziak, L. K., Kuburas, A., Kutschke, W. J., & Russo, A. F. (2020). Vascular actions of peripheral CGRP in migraine-like photophobia in mice. *Cephalalgia, 40*(14), 1585-1604. doi:10.1177/0333102420949173

McGrath, J. C., & Lilley, E. (2015). Implementing guidelines on reporting research using animals (ARRIVE etc.): new requirements for publication in BJP. *Br J Pharmacol, 172*(13), 3189-3193. doi:10.1111/bph.12955

Neuhauser, H., Leopold, M., von Brevern, M., Arnold, G., & Lempert, T. (2001). The interrelations of migraine, vertigo, and migrainous vertigo. *Neurology, 56*(4), 436-441. Retrieved from http://www.ncbi.nlm.nih.gov/pubmed/11222783

Neuhauser, H. K. (2007). Epidemiology of vertigo. *Curr Opin Neurol, 20*(1), 40-46. doi:10.1097/WCO.0b013e328013f432

Neuhauser, H. K. (2009). [Epidemiology of dizziness and vertigo]. *Nervenarzt, 80*(8), 887-894. doi:10.1007/s00115-009-2738-9

Noseda, R., Schain, A. J., Melo-Carrillo, A., Tien, J., Stratton, J., Mai, F., . . . Burstein, R. (2020). Fluorescently-labeled fremanezumab is distributed to sensory and autonomic ganglia and the dura but not to the brain of rats with uncompromised blood brain barrier. *Cephalalgia, 40*(3), 229-240. doi:10.1177/0333102419896760

Paige, C., Plasencia-Fernandez, I., Kume, M., Papalampropoulou-Tsiridou, M., Lorenzo, L. E., David, E. T., . . . Price, T. J. (2022). A Female-Specific Role for Calcitonin Gene-Related Peptide (CGRP) in Rodent Pain Models. *J Neurosci, 42*(10), 1930-1944. doi:10.1523/JNEUROSCI.1137-21.2022

Quirk, W. S., Seidman, M. D., Laurikainen, E. A., Nuttall, A. L., & Miller, J. M. (1994). Influence of calcitonin-gene related peptide on cochlear blood flow and electrophysiology. *Am J Otol, 15*(1), 56-60. Retrieved from https://www.ncbi.nlm.nih.gov/pubmed/8109632

Rea, B. J., Wattiez, A. S., Waite, J. S., Castonguay, W. C., Schmidt, C. M., Fairbanks, A. M., . . . Russo, A. F. (2018). Peripherally administered calcitonin gene-related peptide induces spontaneous pain in mice: implications for migraine. *Pain, 159*(11), 2306-2317. doi:10.1097/j.pain.0000000000001337

Recober, A., Kuburas, A., Zhang, Z., Wemmie, J. A., Anderson, M. G., & Russo, A. F. (2009). Role of calcitonin gene-related peptide in light-aversive behavior: implications for migraine. *J Neurosci, 29*(27), 8798-8804. doi:10.1523/JNEUROSCI.1727-09.2009

Russo, A. F. (2015). Calcitonin gene-related peptide (CGRP): a new target for migraine. *Annu Rev Pharmacol Toxicol, 55*, 533-552. doi:10.1146/annurev-pharmtox-010814-124701

Russo, C. V., Saccà, F., Braca, S., Sansone, M., Miele, A., Stornaiuolo, A., & De Simone, R. (2023). Anti-calcitonin gene-related peptide monoclonal antibodies for the treatment of vestibular migraine: A prospective observational cohort study. *Cephalalgia, 43*(4), 03331024231161809. doi:10.1177/03331024231161809

Tian, R., Zhang, Y., Pan, Q., Wang, Y., Wen, Q., Fan, X., . . . Zhou, J. (2022). Calcitonin gene-related peptide receptor antagonist BIBN4096BS regulates synaptic transmission in the vestibular nucleus and improves vestibular function via PKC/ERK/CREB pathway in an experimental chronic migraine rat model. *J Headache Pain, 23*(1), 35. doi:10.1186/s10194-022-01403-1

Walia, A., Lee, C., Hartsock, J., Goodman, S. S., Dolle, R., Salt, A. N., . . . Rutherford, M. A. (2021). Reducing Auditory Nerve Excitability by Acute Antagonism of Ca(2+)-Permeable AMPA Receptors. *Front Synaptic Neurosci, 13*, 680621. doi:10.3389/fnsyn.2021.680621

Warfvinge, K., & Edvinsson, L. (2019). Distribution of CGRP and CGRP receptor components in the rat brain. *Cephalalgia, 39*(3), 342-353. doi:10.1177/0333102417728873

Zhang, Y., Zhang, Y., Tian, K., Wang, Y., Fan, X., Pan, Q., . . . Zhou, J. (2020). Calcitonin gene-related peptide facilitates sensitization of the vestibular nucleus in a rat model of chronic migraine. *J Headache Pain, 21*(1), 72. doi:10.1186/s10194-020-01145-y

Figure Legends:

Fig. 1. ***A,*** Schematic illustrating mouse setup for VsEP/ABR recordings captured during baseline (control) and 20-30 minutes after intraperitoneal (IP) injections of either PBS as the vehicle or 0.1 mg/kg CGRP in male (M) and female (F) C57BL/6J mice**.** ***B-C,*** Representative click-evoked ABR waveforms - in duplicate -were collected for ABR at a maximal intensity of 100 dB SPL, and waves were labeled (wave1 – wave 4). ***D-E,*** Likewise, representative VsEP waveforms were collected at +6 dB re: 1 g/ms having three, labeled response peaks (p1, n1, and p2). Orange and blue colors are used to distinguish female and male tracings post-CGRP, respectively. The following symbols and colors are used: female - orange, male - square, control - open, CGRP - closed. Sample sizes list - ABR (n = 6F/7M), VsEP (n = 6F/8M). ***G & J,*** Before/after plots indicate the change in amplitude post-CGRP compared to a control response normalized to zero. ***F-G***, A significant increase is seen in wave 1 ABR amplitudes post CGRP for female only, and also when sexes are pooled. ***I-J,*** For VsEPs, a statistically significant decrease in P1-N1 VsEP amplitudes was seen in males only and when sexes were pooled, whereas a trend was seen in females only. IP CGRP had no significant effects on ***(H)*** ABR (wave 2-1) or ***(K)*** VsEP latencies. *$p < 0.05$*, $p < 0.01$**, $p < 0.001$***, $p < 0.0001$*****

Fig. 2. Systemic CGRP increases Acoustic Startle Responses (ASR) in both quiet and background noise, suggesting increased sound sensitivity. ***A,*** Schematic of startle stimulus presented in otherwise quiet background conditions. ***B-C***, in female mice (***B***, n = 6), and male mice (***C***, n=6), there were significant differences between vehicle and IP CGRP ASR measures in quiet conditions ($p < 0.0001$). All mice were more sensitive to the same sound level of ASR stimulus after being injected with CGRP. ***D,*** Schematic of startle stimulus embedded in continuous 60dB SPL broadband background noise. ***E-F*****,** ASR embedded in noise was also more sensitive to same sound level after CGRP injection as shown for female mice (***E***, n = 6), male mice (***F***, n = 6), ($p < 0.001$). All mice were more sensitive to the same level of ASR stimulus whether delivered in quiet or in BBN after being injected with CGRP. Moreover, all mice showed ASR increases with sound level from 80 to 130dB SPL with near maximal startle is elicited by 130 dB SPL stimulus levels. Error bars are SEMs.

Fig. 3. CGRP and Vestibular Challenge increase postural sway in female mice. Symbols and colors are depicted in a similar scheme as previous figures. ***A,*** Timeline involved mice being assessed for effects of IP PBS or IP CGRP on day 1 or day 5, respectively. A 5-minute orbital rotation (125 rpm for 5 minutes, orbital radius = 1 cm) was used as the vestibular challenge, and mice were repeatedly tested (n = 14F/10M). ***B-C,*** Group 95% ellipse areas during pre-VC testing were computed to be 0.50 ± 0.06 cm^2 for females and 0.40 ± 0.04 cm^2 for males. ***D,*** A toy mouse was measured to be 0.02 ± 0.0005 cm^2 for comparison with live animals. ***E,*** IP CGRP increased female postural sway but had little effect in males. ***F,*** Females exhibit greater sway after vestibular challenge and after vehicle injection. ***G,*** Before-after plot is shown to depict changes in sway in repeatedly tested animals. ***H-I,*** Prior to the VC, IP CGRP induced longer AP and ML ellipse lengths in females than was observed during their IP vehicle testing. In addition in females, the vestibular challenge was observed to induce longer AP and ML lengths during IP vehicle testing but not after IP CGRP***,*** which is consistent with CoP area changes***.*** *$p < 0.05$*, $p < 0.01$**, $p < 0.001$***, $p < 0.0001$*****

Supplementary Fig. 1. IP PBS (vehicle) was assessed for ABR (n = 4F/4M) and VsEP (n = 5M/4F) amplitude and latency responses. Females = circles, males = squares, and females + males = diamonds. Open circles indicate control measurements taken before the vehicle was administered, and post-vehicle measurements were taken 20 to 30 minutes after IP administration. One-tailed t-tests were used to assess differences in amplitudes between control (baseline) and post-vehicle for ABR (***A***) and VsEP (***D***). ***B&E***, The Δ change from control to post-vehicle for wave 1 ABR and P1-N1 amplitudes are represented as before-after plots. ***C&F***, Two-way RM ANOVAs were used to compare latency differences for ABR and VsEPs, but no differences were observed.

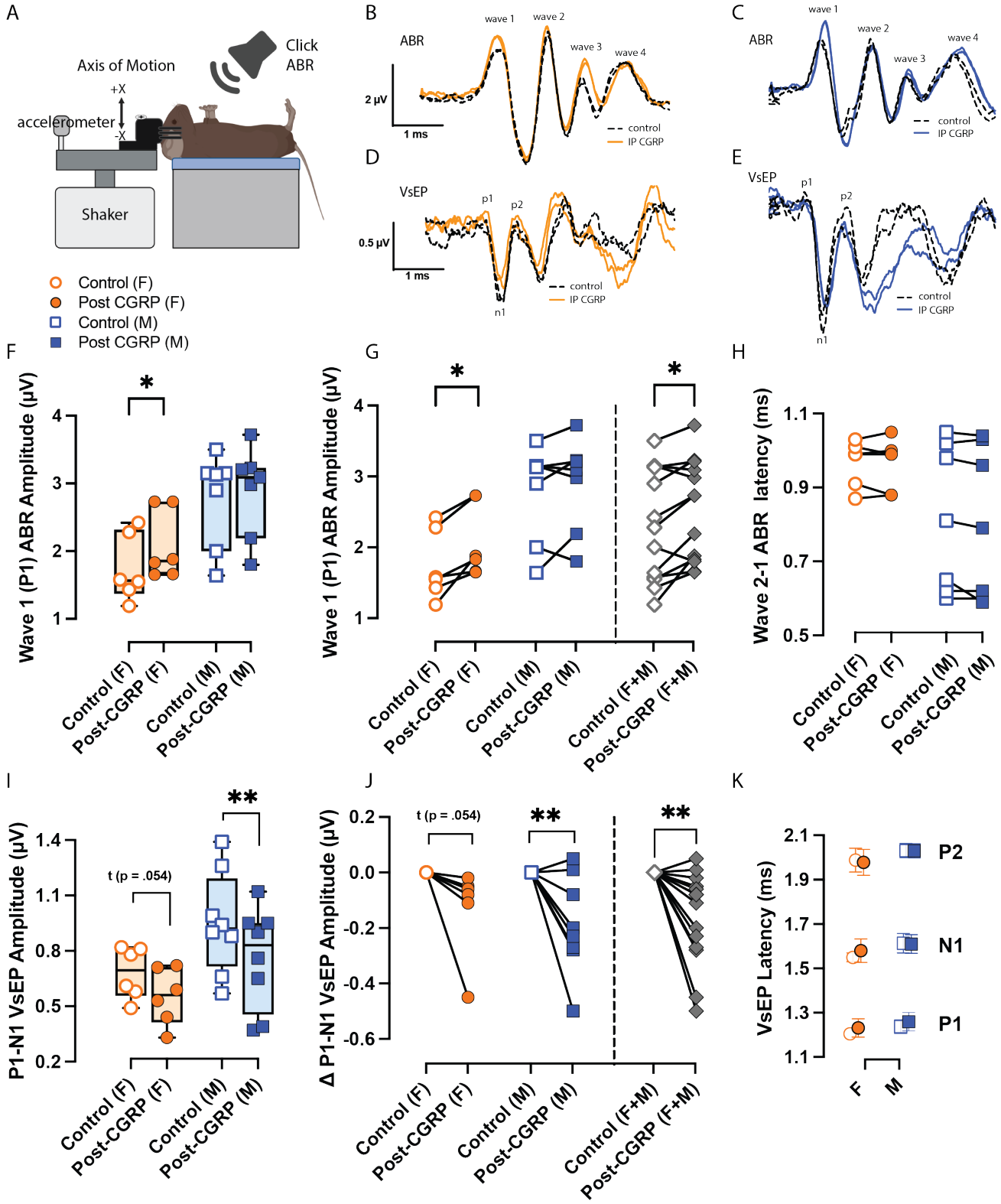
A
Click
ABR
Axis of Motion
+X
accelerometer
-X
Shaker
Control (F)
Post CGRP (F)
Control (M)
Post CGRP (M)
B
ABR
wave 1
wave 2
wave 3
wave 4
2 µV
1 ms
control
IP CGRP
C
ABR
wave 1
wave 2
wave 3
wave 4
control
IP CGRP
D
VsEP
p1
p2
n1
0.5 µV
1 ms
control
IP CGRP
E
VsEP
p1
p2
n1
control
IP CGRP
F
Wave 1 (P1) ABR Amplitude (µV)
Control (F)
Post-CGRP (F)
Control (M)
Post-CGRP (M)
G
Wave 1 (P1) ABR Amplitude (µV)
Control (F)
Post-CGRP (F)
Control (M)
Post-CGRP (M)
Control (F+M)
Post-CGRP (F+M)
H
Wave 2-1 ABR latency (ms)
Control (F)
Post-CGRP (F)
Control (M)
Post-CGRP (M)
I
P1-N1 VsEP Amplitude (µV)
t (p = .054)
Control (F)
Post-CGRP (F)
Control (M)
Post-CGRP (M)
J
Δ P1-N1 VsEP Amplitude (µV)
t (p = .054)
Control (F)
Post-CGRP (F)
Control (M)
Post-CGRP (M)
Control (F+M)
Post-CGRP (F+M)
K
VsEP Latency (ms)
P2
N1
P1
F
M

Fig. 1

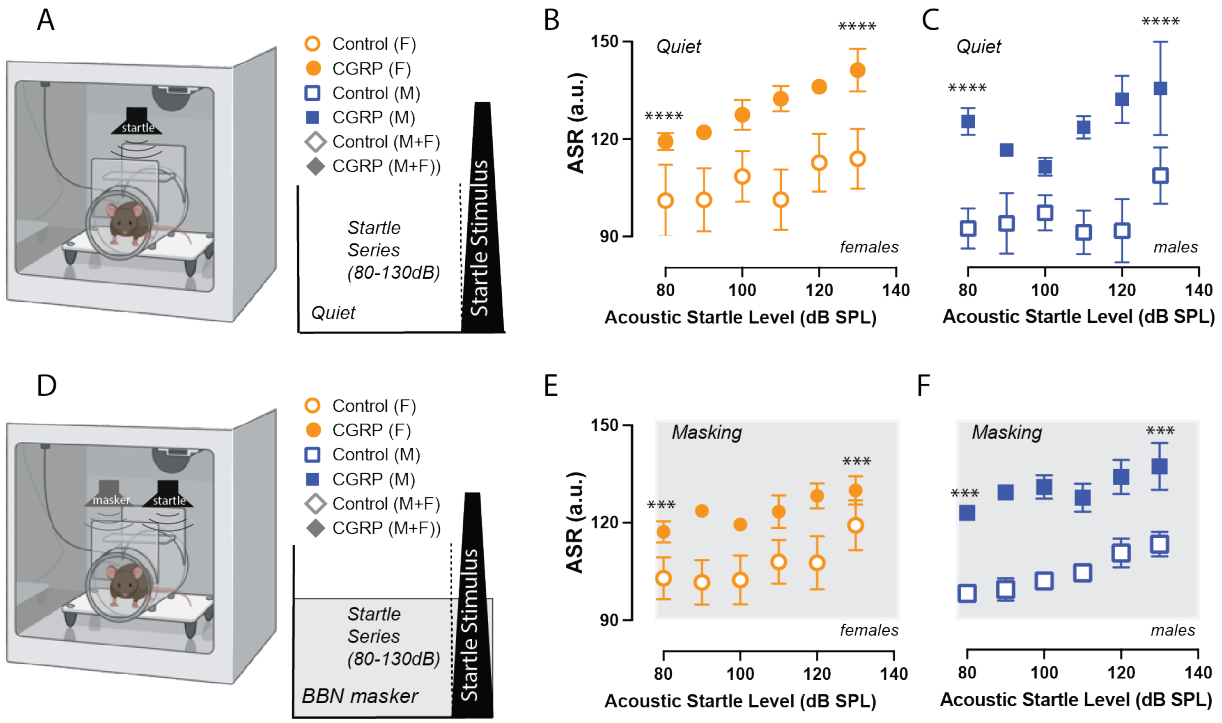
A
startle
Control (F)
CGRP (F)
Control (M)
CGRP (M)
Control (M+F)
CGRP (M+F))
Startle Series (80-130dB)
Quiet
Startle Stimulus
B
Quiet
ASR (a.u.)
150
120
90
****
****
females
80
100
120
140
Acoustic Startle Level (dB SPL)
C
Quiet
****
****
males
80
100
120
140
Acoustic Startle Level (dB SPL)
D
masker
startle
Control (F)
CGRP (F)
Control (M)
CGRP (M)
Control (M+F)
CGRP (M+F))
Startle Series (80-130dB)
BBN masker
Startle Stimulus
E
Masking
ASR (a.u.)
150
120
90
***
***
females
80
100
120
140
Acoustic Startle Level (dB SPL)
F
Masking
***
***
males
80
100
120
140
Acoustic Startle Level (dB SPL)

Fig. 2

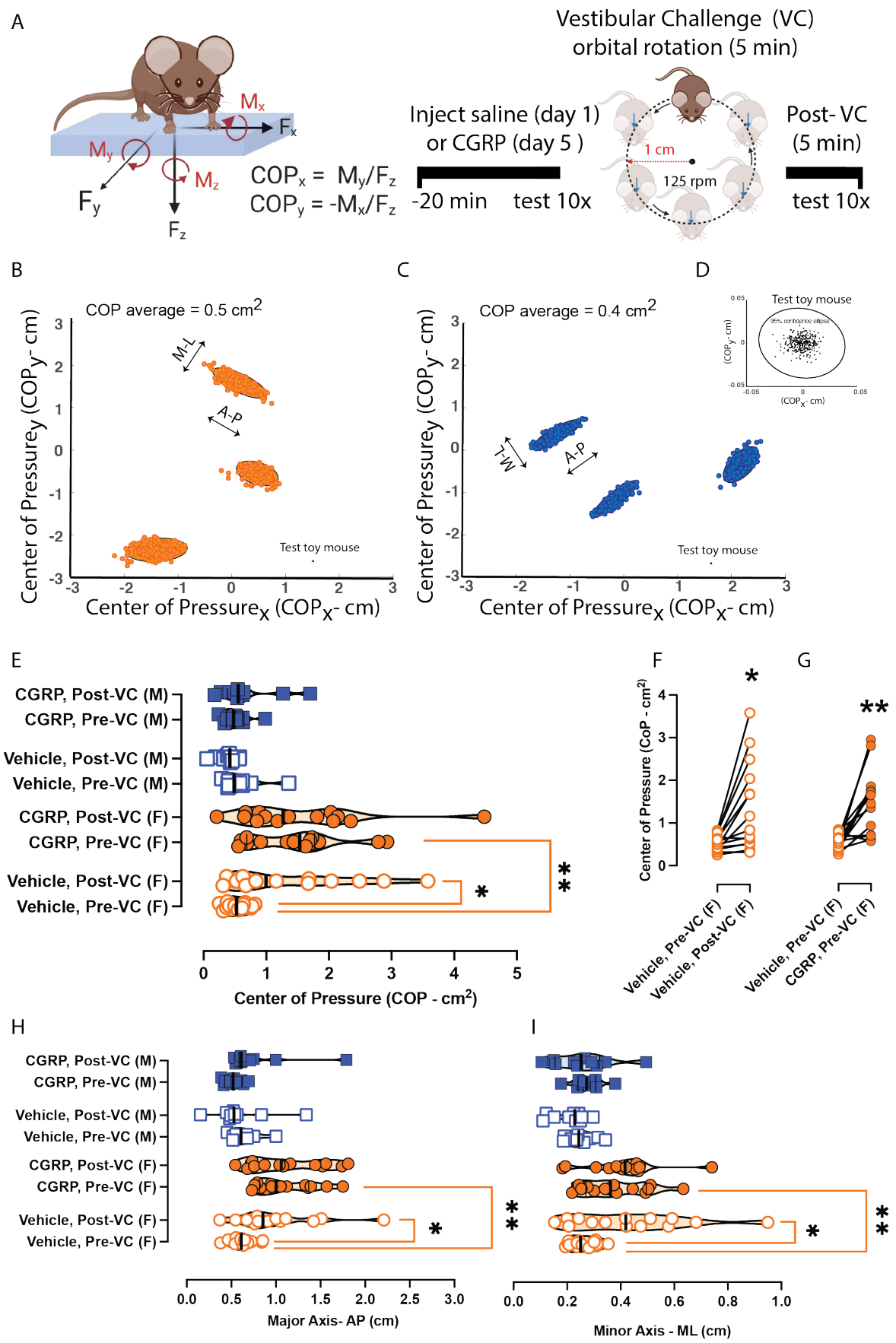
A
Vestibular Challenge (VC)
orbital rotation (5 min)
Mx
Fx
My
Mz
Fy
Fz
COPx = My/Fz
COPy = -Mx/Fz
Inject saline (day 1)
or CGRP (day 5)
-20 min
test 10x
1 cm
125 rpm
Post- VC
(5 min)
test 10x
B
COP average = 0.5 cm2
M-L
A-P
Test toy mouse
Center of Pressure y (COPy- cm)
Center of Pressure x (COPx- cm)
C
COP average = 0.4 cm2
M-L
A-P
Test toy mouse
Center of Pressure y (COPy- cm)
Center of Pressure x (COPx- cm)
D
Test toy mouse
95% confidence ellipse
(COPy- cm)
(COPx- cm)
E
CGRP, Post-VC (M)
CGRP, Pre-VC (M)
Vehicle, Post-VC (M)
Vehicle, Pre-VC (M)
CGRP, Post-VC (F)
CGRP, Pre-VC (F)
Vehicle, Post-VC (F)
Vehicle, Pre-VC (F)
Center of Pressure (COP - cm2)
F
Center of Pressure (CoP - cm2)
Vehicle, Pre-VC (F)
Vehicle, Post-VC (F)
G
Vehicle, Pre-VC (F)
CGRP, Pre-VC (F)
H
Major Axis- AP (cm)
I
Minor Axis - ML (cm)

Fig. 3

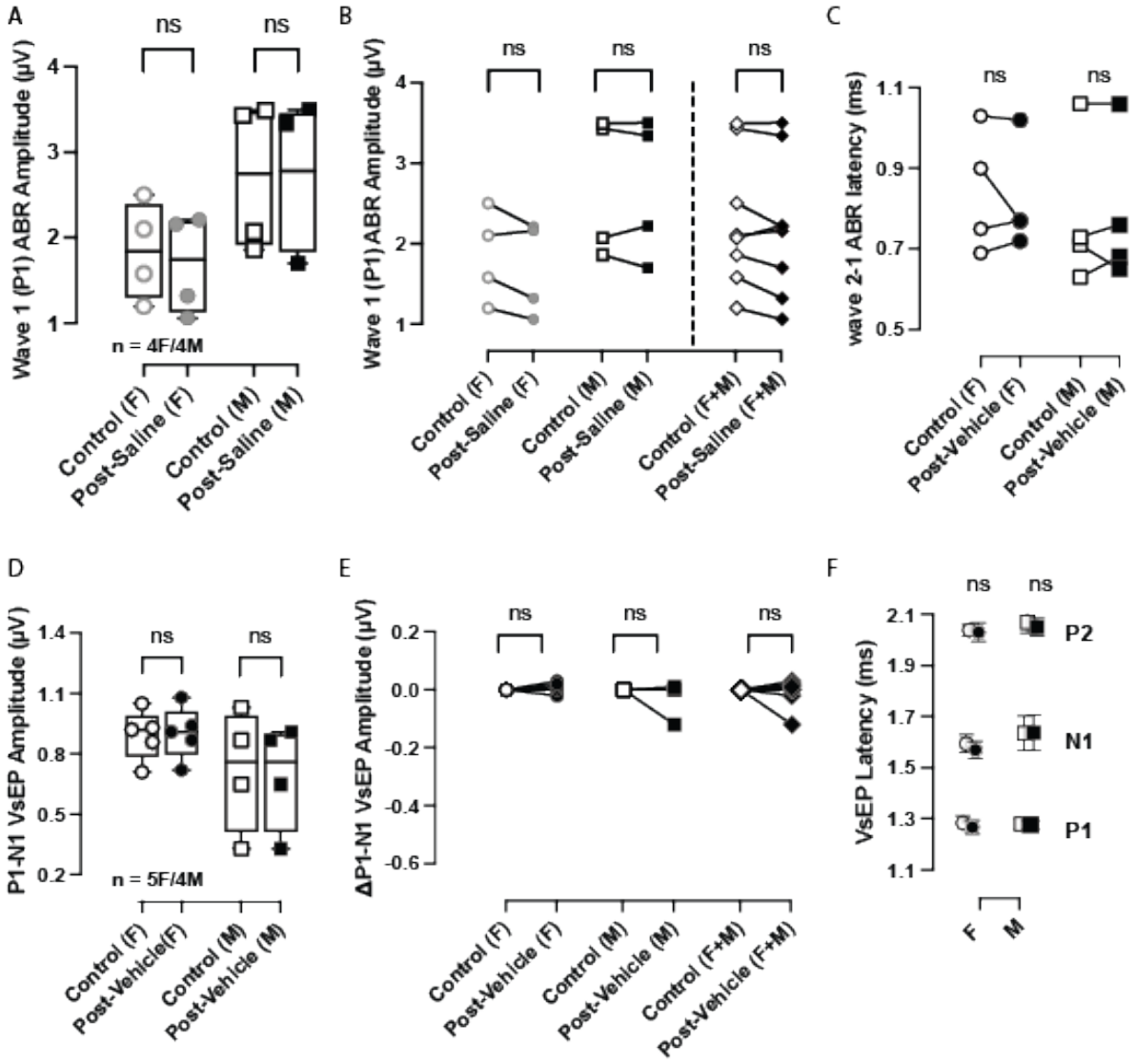

Supplementary Fig. 1